Journal of Materials Chemistry C

PAPER

View Article Online
View Journal | View Issue

Cite this: J. Mater. Chem. C, 2014, 2, 7589

Robust optical oxygen sensors based on polymer-bound NIR-emitting platinum(II)–benzoporphyrins†

L. H. Hutter,‡[a] B. J. Müller,‡[b] K. Koren,[c] S. M. Borisov*[b] and I. Klimant[b]

Received 12th May 2014
Accepted 16th July 2014

DOI: 10.1039/c4tc00983e

www.rsc.org/MaterialsC

Several advanced optical oxygen sensor materials are presented. They are based on bright NIR-emitting platinum(II)–benzoporphyrins covalently incorporated into a variety of polymeric matrices. The dye–polymer conjugates are prepared either *via* Suzuki coupling of the brominated porphyrins to the styrene backbone or *via* co-polymerisation of the monomers with monostyryl porphyrin derivative. Importantly, in both strategies a highly stable C–C bond is obtained. The resulted materials benefit from excellent photophysical properties of the benzoporphyrin dyes (high brightness, emission in the NIR part of the spectrum) and high stability of the covalently grafted materials due to complete suppression of dye migration and leaching. This is demonstrated to be particularly important for operation of the sensors in harsh conditions *e.g.* during steam sterilization where the materials based on non-covalently grafted dyes showed significant drift of their calibration. Additionally, we present a new synthetic method for preparation of analytically pure benzoporphyrins *via* simple 1-step template condensation which a promising alternative to the commonly used Lindsey method.

Introduction

Optical oxygen sensors constitute widely-used analytical tools which are applied, for example, for the study of cellular function,[1,2] in medical diagnostics,[3,4] marine biology,[5] food packaging[6,7] and for process monitoring in industry and biotechnology.[8] In a general layout a phosphorescent indicator dye is physically entrapped into a matrix material which is a polymer (polystyrene, poly(methylmethacrylate), silicone, or ethylcellulose and their derivatives[9,10]) or a sol–gel.[11,12] The matrix acts as a solvent and a support for the dye, as a permeation-selective barrier for the interfering chemical species and it also controls oxygen permeability. A suitable matrix can enhance both the specificity and selectivity of the sensor as well as its stability over time. A variety of oxygen indicators has been developed over the past decades[13] since the photophysical properties of the dyes have to be adjusted for a particular application. The development of dyes that are excitable in the red and NIR part of the electromagnetic spectrum has been of particular interest in recent years.[14] These indicator dyes are well suited for measurements in autofluorescent or highly scattering media, such as *in vivo* samples in many bioanalytical applications. Oxygen indicators based on platinum(II) and palladium(II) complexes of porphyrin ketones[15] and porphyrin lactones,[16] and particularly of pi-extended benzo- and naphthoporphyrins[17–19] and related compounds[20] were found to be particularly promising for sensing applications. With the exception of water-dispersible oxygen-sensitive dendrimers (representing self-contained analytical tools primarily for imaging applications)[21,22] the above indicators are physically entrapped in a suitable polymeric matrix. Major restrictions of this approach are determined by the level of chemical and physical interaction between the indicator and its local environment. Low solubility of the indicator in the sensor matrix gives rise to leaching and aggregation; both processes seriously compromise the performance of an optical oxygen sensor over time. A lipophilic indicator will unlikely leach out of the sensor in aqueous environment but it may slowly migrate into the hydrophobic sensing support such as the very popular polyethylene terephthalate. Such migration processes are greatly accelerated at elevated temperatures, *e.g.* during steam sterilization of the sensors. Leaching can be particularly critical for materials with large surface to volume ratio, such as oxygen-sensitive nanoparticles. Covalent immobilisation of the indicators into polymeric matrices represents the optimal strategy to overcome the above limitations. Oxygen sensing materials based on covalently grafted iridium(III)[23,24] ruthenium(II)[25–28] and platinum(II) or palladium(II) complexes[29–33] were reported. The *meso*-tetra(pentafluorophenyl) porphyrin (TFPP) complexes,

[a]Department of Biochemistry, University of Oxford, South Parks Road, OX1 3QU, UK
[b]Institute for Analytical Chemistry and Food Chemistry, Graz University of Technology, Stremayrgasse 9, A-8010 Graz, Austria. E-mail: sergey.borisov@tugraz.at
[c]Marine Biological Laboratory, University of Copenhagen, Strandpromenaden 5, DK-3000 Helsingør, Denmark

† Electronic supplementary information (ESI) available. See DOI: 10.1039/c4tc00983e

‡ These authors contributed equally to this work.

particularly, can be easily modified *via* nucleophilic substitution of the *p*-fluorine atom of the pentafluorophenyl groups.[29–31,33] Significantly higher stability of the new materials compared to the sensors obtained *via* physical entrapment of the dyes was demonstrated.[31] To the best of our knowledge highly promising NIR indicators have not been covalently grafted into oxygen-sensing materials. A versatile immobilisation strategy used for TFPP derivatives is not feasible since the *meso*-tetra(pentafluorophenyl)-tetrabenzoporphyrin complexes does not form readily.[34]

Herein, we present an efficient and versatile strategy towards advanced optical oxygen sensing materials based on platinum(II)-benzoporphyrin complexes covalently incorporated into a variety of relevant matrices. New brominated porphyrins can be either directly attached to the polymers or modified to give reactive monomers. Importantly, the synthetic strategy relies on Suzuki coupling which results in chemically stable C–C bond. It will be demonstrated how the covalent immobilisation improves the performance of the sensor materials compared to conventional sensors. In addition we will present a new efficient method for the synthesis of benzoporphyrins *via* template condensation which, compared to the previous reports, results in analytically pure products.

Results and discussion

Synthesis of the brominated Pt(II)–porphyrin indicators

Brominated Pt(II)–benzoporphyrins serve as a synthetic platform for the covalent immobilisation of the indicator dye in various polymer matrices *via* Suzuki coupling. Depending on immobilisation strategy either tetra- or mono-substituted derivates can be used (Fig. 1). The tetra-substituted Pt(II) benzoporphyrin was initially synthesized using an adapted standard protocol.[35,36] This involved Lindsey-condensation[37] of 4,5,6,7-tetrahydroisoindole with 4-bromobenzaldehyde yielding compound **A1**, the subsequent platination of the product (**A2**) and finally oxidation of the cyclohexene rings to yield the benzoporphyrin **3a**. Surprisingly, the solubility of **A1** was found to be rather low and the dye aggregated readily in organic solvents. On the other side, solubility of various metal-free tetraphenyltetracyclohexenoporphyrins, their Pt(II) complexes and the respective benzoporphyrins is known to be rather good.[34,36] The bromine atoms in the *para*-position of the *meso*-substituted phenyl rings appear to promote aggregation of the dyes. Due to low solubility of **A1** in organic solvents, purification of the product was challenging; hence the crude product was used in the next step after removal of the solvent.

In the second step, platination was performed in trimethylbenzene using $Pt(C_6H_5CN)_2Cl_2$ as a precursor complex, which is a modification of the method published previously.[38] Trimethylbenzene allows for relatively high reaction temperatures (and therefore fast metalation) but in contrast to diphenylether can be easily removed under reduced pressure.

In the final step, the brominated benzoporphyrin **3a**, was obtained *via* oxidation of **A2** with 2,3-dicyano-5,6-dichlorobenzoquinone (DDQ). Similarly to **A1**, the solubility of the Pt(II)

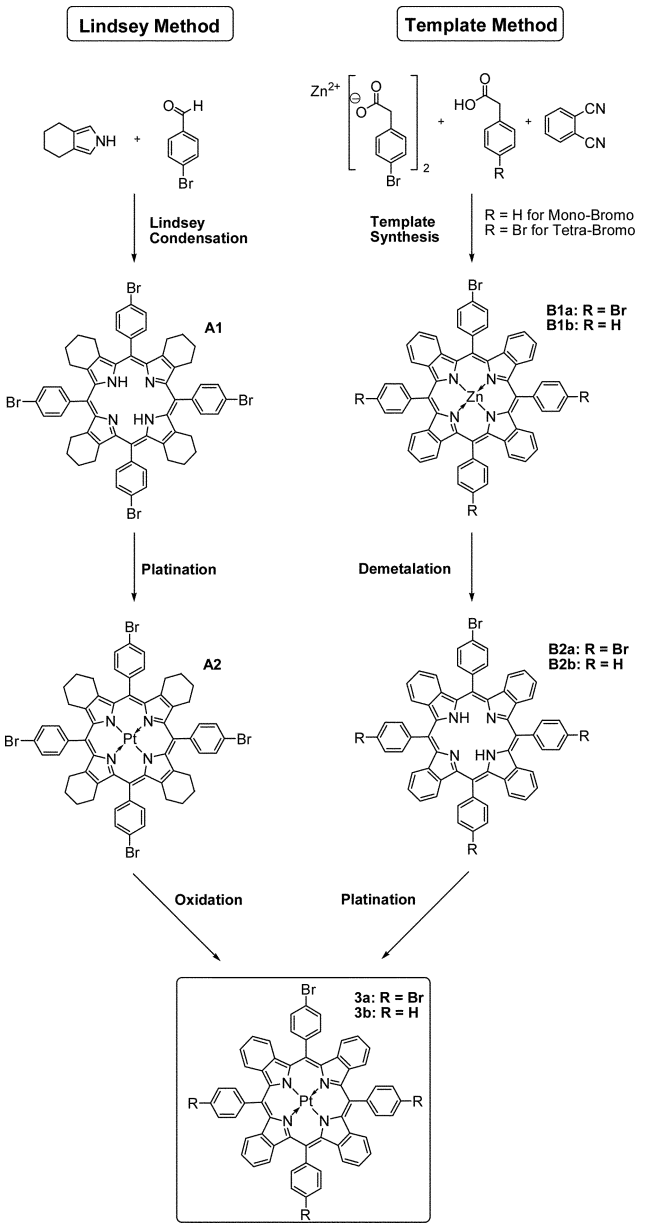

Fig. 1 Synthetic approaches towards reactive bromo-modified Pt(II)–benzoporphyrins – commonly used Lindsey condensation (left) and a modified template-method (right). Tetra-substituted porphyrin $PtTPTBPBr_4$ was synthesized using both methods. Mono-substituted dye PtTPTBPBr was prepared using template-method.

benzoporphyrin was rather poor. The purification was possible only for diluted solutions.

One of the drawbacks of the above method is that it relies on 4,5,6,7-tetrahydroisoindole which is synthesised from not inexpensive ethyl isocyanoacetate. Template condensation represents an alternative method yielding Pt(II) benzoporphyrins in only 3 simple steps, starting from very cheap phthalimide and phenylacetic acid. However, the template condensation was reported to yield a number of benzyl-substituted side products which are extremely challenging to separate.[38,39] Preliminary experiments indicated that the condensation of phthalimide with 4-bromophenylacetic acid instead of phenylacetic acid

resulted in a low yield of the zinc benzoporphyrin. Herein we present a new efficient method to yield analytically pure benzoporphyrins (Fig. 1). By substituting phthalimide with dicyanobenzene, the reaction temperature could be reduced from 350 °C to 280 °C which greatly enhanced the yield of zinc tetra(4-bromophenyl)tetrabenzoporphyrin. The yield of the target compound after chromatographic purification was 6% which is rather good considering the low cost of the starting materials and simplicity of the procedure. Based on this novel protocol we were able to synthesize $PtTPTBPBr_4$ (compound **3a**) in only three steps. The Pt(II) complex can be conveniently obtained after demetalation of the respective zinc porphyrin and subsequent platination of the metal-free porphyrin. The ^1H NMR analysis and mass spectroscopic investigation indicate that no other porphyrin derivatives are formed and the product is identical to that obtained *via* Lindsey method. Considering high potential of zinc[40] and platinum(II) benzoporphyrins[41] for energy conversion applications the new method is expected to be particularly promising for simple and cost-efficient synthesis of these sensitizers. Many other commercially available dicyanobenzenes and phenylacetic acid derivatives can be used to provide necessary functionalities.

Mono-brominated Pt(II) porphyrin (**3b**) is also of great practical interest for covalent immobilisation since it only has a single site suitable for modification and hence does not act as cross-linker when it becomes incorporated into a polymer. The respective zinc complex was obtained *via* the modified template condensation using a mixture of phenylacetic- and 4-bromophenylacetic acids. As determined by MALDI-TOF, this approach results in a mixture of products with a degree of bromo-substitution ranging from 0 to 2 (Fig. S6†). Chromatographic separation of these extremely similar compounds is virtually impossible. Due to bad ionization of the bromo-functionalized complexes, we were not able to reliably determine the contributions of the individual forms at this stage. However, as will be demonstrated in the following, a mixture of the mono-, dibromo- and unsubstituted porphyrins is suitable for preparation of soluble materials.

Photophysical properties

Fig. 2 compares the absorption and emission spectra of the new brominated porphyrin dyes with those of the non-substituted dye. Evidently, the substitution has a very minor effect on the spectral properties of the dyes. A small bathochromic shift of the Q-band is observed for PtTPTBPBr (**3b**) and $PtTPTBPBr_4$ (**3a**) compared to PtTPTBP (1 and 5 nm, respectively). Similarly, the corresponding emission spectra shift bathochromically by 2 nm and 9 nm, respectively. Despite potential quenching of the "heavy" bromine atoms we did not observe any significant change in the luminescence decay times and luminescence quantum yields upon bromination (Fig. 2). This correlates well to the results of Zhao and co-workers who demonstrated that the heavy atom effect of the halogen atoms in structurally related BODIPY dyes is much less efficient if they are positioned far away from the π-conjugated core of the chromophore.[42]

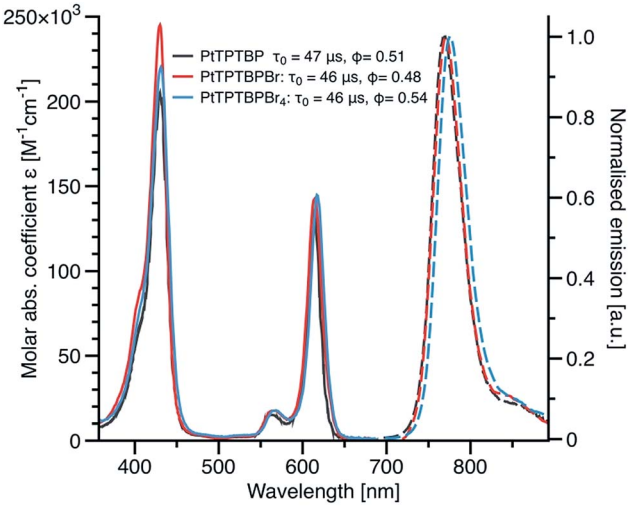

Fig. 2 Absorption (in dichloromethane) and emission spectra (in deoxygenated toluene) for the new Pt(II)-benzoporphyrin complexes.

The photostability of the dye is of particular interest for practical applications; especially in those cases where high light densities are used or measurements are performed for prolong time. $PtTPTBPF_4$ which has excellent photostability[34] was used for comparison. The photostability of the new compounds was found to be similar to that of $PtTPTBPF_4$.

Preparation of the porphyrin–polymer composites

In order to covalently couple the indicators to the sensor matrix, two different strategies were used (Fig. 3). Both rely on Suzuki coupling and result in chemically stable C–C bonds. In the first approach, polystyrene bearing different amounts of boronic acid residues (Table S1 ESI†) were prepared by co-polymerisation of styrene and 4-vinylphenylboronic acid (**4**). The tetra- or mono-brominated Pt(II) benzoporphyrin was attached to the polymer in one step. The limitation of the approach is that the amount of the incorporated boronic acid groups is not easy to control and is lower than theoretically expected (*e.g.* 0.07 instead of 0.1 mol%). In order to avoid cross-linking when using the tetra-brominated porphyrin it should be used in excess to saturate all the boronic acid groups. The unbound dye is then removed during purification of the polymer.

In the second strategy, the mono-brominated dye was reacted with 4-vinylphenylboronic acid to produce reactive dye monomer (**5**). Using a standard protocol for Suzuki-coupling reactions, we were able to achieve acceptable yields of about 50% for the styryl-modified benzoporphyrin. The Heck reaction with the vinyl group of the boronic acid leads to the major side product. Due to the polarity of the boronic acid residue, the reactant as well as the side product could be readily removed by means of column chromatography. MALDI-TOF data (Fig. S7†) indicate a mixture of PtTPTBP, PtTPTBPStyr and $PtTPTBPStyr_2$ (ratio 80 : 100 : 55) which is likely to reflect the substitution pattern of the respective brominated complexes. Relatively high content of unmodified PtTPTBP and the di-substituted

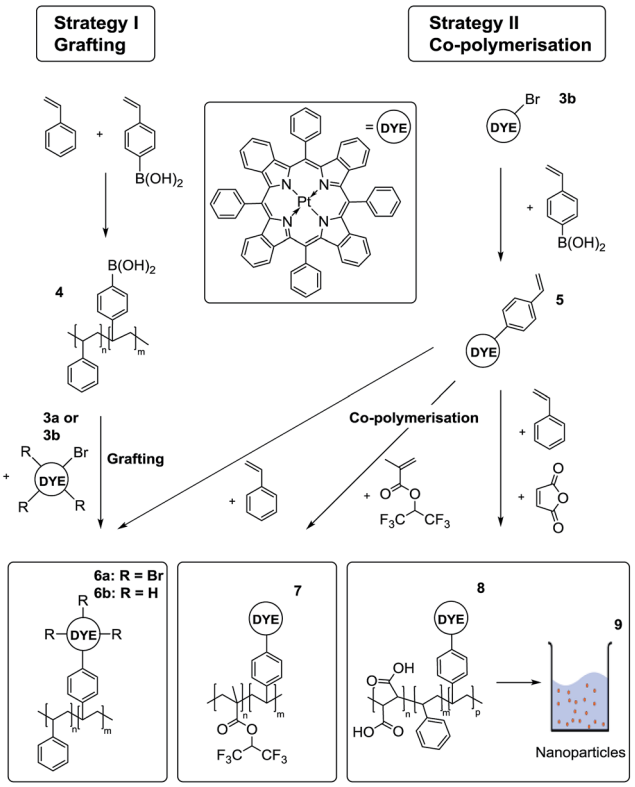

Fig. 3 Two different strategies for covalent immobilisation of Pt(II)–benzoporphyrins based on C–C Suzuki-cross-coupling reaction. A co-polymer with boronic acid groups (**4**) can be used for covalent grafting of either using tetra- (**3a**) or monobromo- (**3b**) substituted benzopophyrin. In the second strategy, the indicator is modified with styryl groups (**5**) and subsequent polymerisation with a variety of monomers is performed (styrene (**6b**), 1,1,1,3,3,3-hexafluoroisopropylmethacrylate (**7**) or maleic anhydride and styrene (**8**)). The latter can be used for the preparation of water dispersible nanoparticles (**9**).

porphyrin in this mixture of products is not crucial for the subsequent co-polymerisation reactions since the unbound dye is removed in the purification process and the disubstituted porphyrin dye does cause significant cross-linking due to rather low concentrations used.

Oxygen-sensitive polymers were obtained by co-polymerisation of different monomers with the styrene-modified dye, using radical polymerisation with AIBN as initiator. Reactions towards material **6b** and **8** where carried out without solvent resulting in polymers with high PDI values, ranging from 1.20 to 5.44. These PDI values are not likely to have major influence on the properties of the sensor. 1,1,1,3,3,3-Hexafluoroisopropyl methacrylate was polymerised in the solution of tetrahydrofuran (THF) as the dye is insoluble in the monomer. In all procedures, unbound indicator was removed *via* precipitation of the polymer in methanol. The precipitation procedure was repeated until no more indicator dye could be found in the solution. In the case of material **8**, functionalized poly(styrene-*co*-maleic acid) particles were obtained by precipitation of a solution of the polymer in THF from water according to the reported procedure.[43]

Overall, the co-polymerisation approach is preferable to the first strategy (grafting) due to its high versatility: the approach can be used for numerous monomers and it warrants a higher degree of control over the amount of indicator incorporated into the polymer.

Properties of the sensing materials

Fig. 4 shows the effect of covalent immobilisation of the indicator on the calibration curve of the sensor (Stern–Volmer plot): PtTPTBPBr physically entrapped in polystyrene is used as a reference for the co-polymerised and grafted sensor materials. All three sensor materials possess similar phosphorescence lifetimes in the absence of oxygen. The sensitivities of all the materials are similar. It appears that the way of dye immobilisation only minor affects the calibration. The decay time plots (Fig. 4) are less linear compared to the luminescence intensity plots (Fig. S8†) which is a typical case for the optical oxygen sensors. In fact, a linear fit almost ideally describes the intensity plots (correlation coefficient $r^2 = 0.9997$), but it is less adequate for the decay time plots ($r^2 = 0.997$). The modified equation from the two-site model[44] adapted for the decay time plots (eqn (1), ESI†) delivers satisfactory results ($r^2 = 0.9996$).

The effect of dye loading on the luminescence lifetime for the grafted sensor materials is shown in Fig. 5. A typical oxygen sensor based on non-covalently entrapped indicator would contain about 1–1.5 wt% of an indicator dye. As can be seen, only slight decrease of the luminescence decay time is visible for a higher concentration of 1.8 wt%. However, the phosphorescence lifetimes become markedly shorter upon further increase of dye loading (50.7, 47.3 and 38.0 μs at 0.33, 1.82 and 6.92 wt%, respectively). This self-quenching is likely to be due to aggregation of the dye at higher dye loadings.

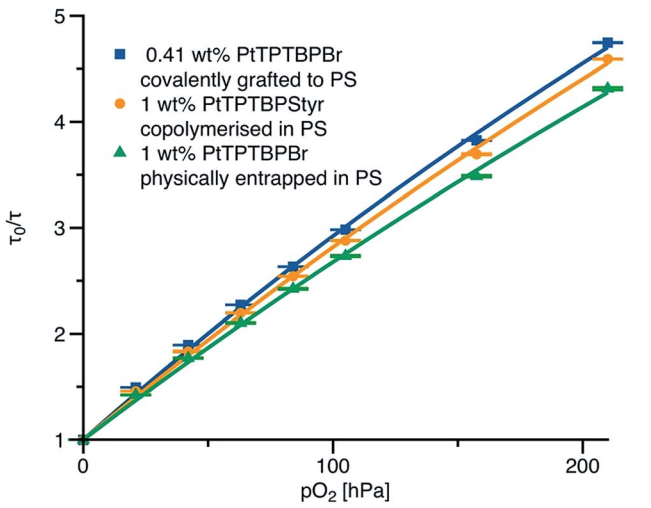

Fig. 4 Stern–Volmer plots for polystyrene-based sensing materials at 25 °C. The fit is performed according to the eqn (1) (ESI†). The fit parameters are: $f = 0.76$, $K_{SV1} = 0.0298$ h Pa^{-1} for covalently grafted PtTPTBPBr; $f = 0.82$, $K_{SV1} = 0.0249$ h Pa^{-1} for co-polymerised PtTPTBPStyr and $f = 0.82$, $K_{SV1} = 0.0228$ h Pa^{-1} for physically entrapped PtTPTBPBr; $K_{SV2} = 0.2K_{SV1}$ in all cases.

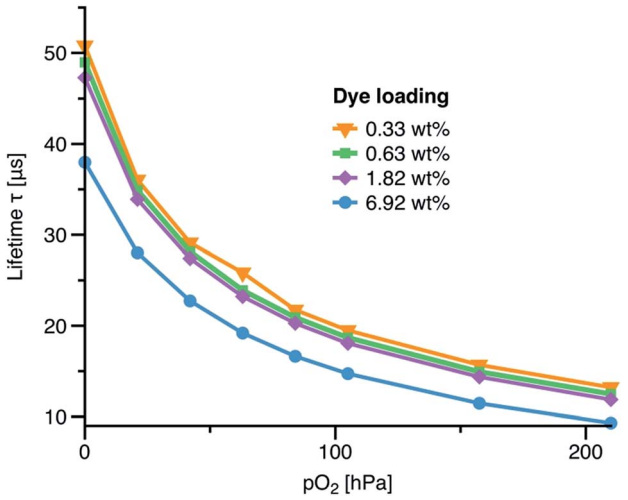

Fig. 5 Calibration plots (at 25 °C) for oxygen sensors based on $PtTPTBPBr_4$ grafted to polystyrene (**6a**) for varying amount of the immobilised indicator.

Importantly, the styryl-modified benzoporphyrin **5** can be easily incorporated in a variety of other polymeric matrixes. Hence, oxygen sensing materials covering a broad range of potential application fields can be produced (Fig. 6). For example, co-polymerisation with hexafluoroisopropyl methacrylate results in significantly more sensitive materials compared to polystyrene-based ones. Thus, this sensor is much better suitable for measurements at low oxygen. It should be mentioned that the same methodology can be adapted for grafting of analogous Pd(II) benzoporpyhrins which possess about 7 times longer phosphorescence decay times.[34] The combination of Pd(II) benzoporphyrins and poly(hexafluoroisopropyl methacrylate) would be suitable for trace oxygen sensing.

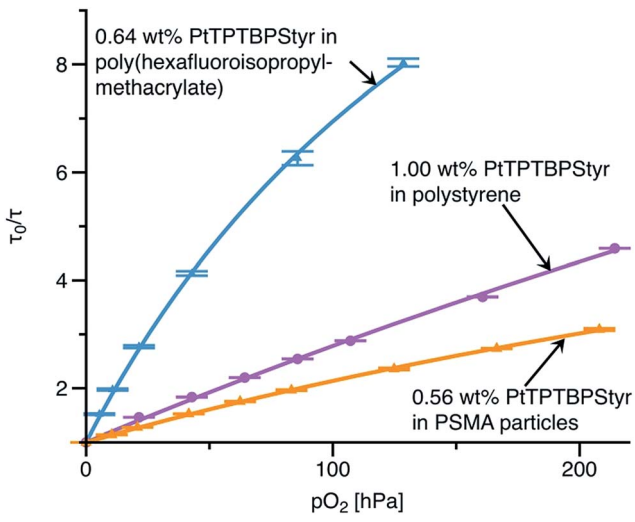

Fig. 6 Stern–Volmer plots for sensing materials based on co-polymerised **5** at 25 °C. The fit parameters are: $f = 0.90$, $K_{SV1} = 0.110$ h Pa^{-1}, $K_{SV2} = 0.0041$ h Pa^{-1} for poly(hexafluoroisopropylmethacrylate; $f = 0.82$, $K_{SV1} = 0.0249$ h Pa^{-1}, $K_{SV2} = 0.0050$ h Pa^{-1} for polystyrene and $f = 0.73$, $K_{SV1} = 0.0183$ h Pa^{-1}, $K_{SV2} = 0.0050$ h Pa^{-1} for PSMA particles.

We also prepared a co-polymer of styrene and maleic acid with co-polymerised Pt(II) benzoporphyrin which was used to prepare nanoparticles *via* precipitation (**9**). The nanosensors (85 nm, PDI = 0.15) are negatively charged at neutral pH (Zeta potential – 40.9 mV) due to hydrolysis of maleic acid anhydride. Oxygen sensitivity is slightly lower than for the polystyrene materials (Fig. 6). Covalent grafting of the indicators in the nanoparticle-based sensors is of particular importance due to their high surface to volume ratio, and therefore intense interaction with the environment (*e.g.* proteins and other species in biological probes). Additionally relatively small diffusion distances in the nanoparticles can aggravate leaching of the non-covalently bound dyes. Our approach overcomes this limitation.

To assess the effect of covalent immobilisation on the long-term performance of the sensor and the ability of covalent immobilisation to suppress effects associated with migration of the indicator dye, we prepared sensor films on glass and polyethylene terephthalate (PET) support foil and exposed them to repeatable autoclave treatment for up to 15 hours at 135 °C. Fig. 7 shows luminescence lifetimes measured under nitrogen and air saturation for the sensor material based on compound **5** co-polymerised with polystyrene compared with corresponding data for compound **3a** physically entrapped in polystyrene. Regardless of the support material the phosphorescence lifetimes under nitrogen are virtually not affected by high temperature and humidity. On the other hand, the decay times under air saturation for the physically entrapped indicator increase dramatically (13.0 to 23.8 µs after 15 h). This effect is caused by the migration of dye into less oxygen-permeable polymeric support. Such a change would result in ~100% error in determination of pO_2 at air saturation after 15 h of autoclavation. Although migration is very fast at elevated temperatures

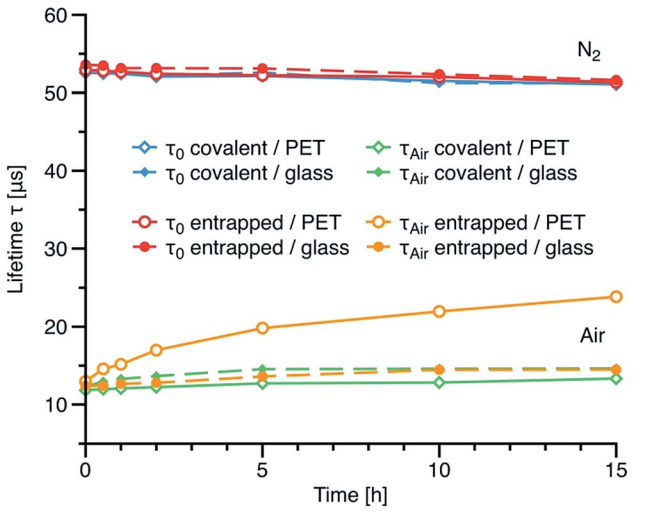

Fig. 7 Influence of autoclavation (135 °C) on the luminescence decay times (at nitrogen and air saturation, measured at 25 °C) of the oxygen sensors based on **6b** and on $PtTPTBPBr_4$ physically entrapped in polystyrene. Two different supports (PET and glass) are compared. The same sensor foils were autoclaved repeatedly throughout the whole experiment.

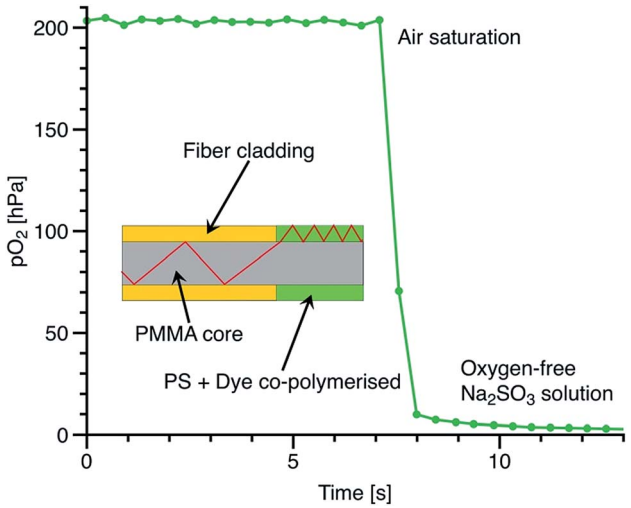

Fig. 8 Cross-section and dynamic response of the fiber-optic oxygen sensor. The excitation light is coupled into a thin sensor layer coated onto the core of a PMMA fiber.

it is expected to be noticeable also at room temperature during prolong storage times. Obviously, the PET support is not suitable for the sensor film based on the physically entrapped dye. For comparison, only very minor increase of the decay time is observed when the non-covalently embedded dye material is coated on glass support. Notably, glass support is less flexible regarding processing and mechanical stability compared to PET. On the contrary, our new materials based on the covalently immobilised dye do not show any significant migration into either supports used. In fact only minor change in the decay times is observed even after 15 h of autoclavation which would produce and error of ~18% in determination of pO_2 at air saturation providing that the sensor is not recalibrated after sterilization. It should be mentioned that 30 min sterilization is typically sufficient and therefore the error in pO_2 quantification is virtually negligible. Thus, the new materials are particularly promising for application in harsh conditions (elevated temperatures, steam sterilization).

Suppressed migration of the covalently immobilised dye allowed us to directly apply the sensor composition to the PMMA fiber in order to obtain cheap and fast responding fiber-optic sensors (Fig. 8). The physically entrapped indicator dyes would migrate into the PMMA core over time and compromise sensor performance. However, in the case of sensor materials incorporating covalently immobilised indicator dyes, direct coating of the PMMA fiber allows for very thin sensor polymer layers without migration issues. The response times of such layers are very fast and are below 1 s.

Conclusions

We presented a simple and versatile strategy for the preparation of high performance oxygen-sensing materials. These materials rely on the NIR emitting bright and photostable Pt(II) benzoporphyrins covalently immobilised into different polymeric matrices. The new sensors overcome the limitations of their predecessors based on physically entrapped dyes. Migration and leaching are completely eliminated which not only ensures the reliable operation of the sensors in harsh conditions (such as elevated temperatures) but also enables higher flexibility of sensor formats (*e.g.* fast responding fiber-optic sensors based on PMMA fibers). We also reported a novel straightforward and inexpensive synthetic route to the template-directed synthesis of (bromo-substituted) Pt(II)–benzoporphyrins. The new method not only allows preparation of reactive bromo-substituted porphyrins available for Suzuki coupling, but also other numerous porphyrins which can be used for a variety of emerging applications such as triplet–triplet annihilation upconversion.

Experimental

Materials

Ethyl isocyanoacetate, 1-nitro-1-cyclohexene, 2,3-dicyano-5,6-dichlorobenzoquinone (DDQ), boron-trifluorid-diethyletherate ($BF_3 \cdot Et_2O$), 1,2,4-trimethylbenzene (TMB), benzonitrile, potassium carbonate (K_2CO_3), styrene, 1,1,1,3,3,3-hexafluoroisopropyl methacrylate, phenylacetic acid, 4-bromophenylacetatic acid, 1,2-dicyanobenzene and water-free dichloromethane (DCM) were purchased from Aldrich. Zinc 4-bromophenylacetate was obtained as a white precipitate in an exchange reaction between zinc acetate and 4-bromophenylacetic acid. 4-Bromobenzaldehyde, 4-vinylboronic acid, tetrakis(triphenylphosphine)palladium(0) ($Pt(PPh_3)_4$) and methanesulfonic acid were from ABCR. Maleic anhydrid and sodium sulfite (Na_2SO_3) were obtained from Fluka. Azobisisobutyronitrile (AIBN), aluminium oxide (neutral, 50–200 μm) (Al_2O_3) and polystyrene (PS) ($Mw = 260\,000$ g mol^{-1}) were purchased from Acros. Poly(ethylene terephthalate) (PET) support Melinex 505 was obtained from Pütz. Nitrogen (99.999% purity) was obtained from Air Liquide. Hydrochloric acid 37% (HCl), sodium sulfate anhydrous (Na_2SO_4) and all other used solvents were from VWR. Zinc(II) oxide (ZnO) and silica-gel 60 (0.063–0.200 mm) were from Merck. Platinum(II) chloride ($PtCl_2$) was obtained from ChemPur. PMMA fibers were obtained from Ratioplast. HPLC grade chloroform, ethyl acetate and water-free dimethylformamide (DMF) were obtained from Roth. 4,5,6,7-Tetrahydroisoindole was synthesized as described elsewhere.[36] The precursor $Pt(C_6H_5CN)Cl_2$ was obtained by stirring $PtCl_2$ in boiling benzonitrile for one hour and precipitating the resulted product with hexane. The yellow product is filtrated, washed with hexane and dried at 60 °C.

Synthetic procedures

Tetra-(4-bromophenyl)-cyclohexenoporphyrin (H_2TPCHPBr$_4$, A1). 4,5,6,7-Tetrahydroisoindole (1.220 g, 0.010 mmol) and 4-bromobenzaldehyde (1.850 g, 0.010 mmol) were dissolved in 1 l of anhydrous DCM, which was first deoxygenated with argon for 40 minutes. The reaction mixture was degassed for 10 minutes. The flask was shielded from light and $BF_3 \cdot Et_2O$ (143 mg, 0.127 ml, 0.001 mmol) was added using a syringe. The reaction mixture was stirred for 3 h at room temperature before adding

0.05 ml additional $BF_3 \cdot Et_2O$ and subsequent stirring for 2 h. DDQ (2.860 g, 0.0125 mmol) was added. The reaction mixture was stirred for 14 h at room temperature. Remaining DDQ was quenched with 10 wt% Na_2SO_3 solution and the organic phase was dried over Na_2SO_4. The solvent was removed by rotary evaporation. The crude product was used in the next step without further purification. Yield: 83% estimated *via* molar absorption coefficient assuming $\varepsilon = 250\,000\ M^{-1}\ cm^{-1}$ for the Soret band at 440 nm. UV-Vis (acetone): λ_{max} (rel. int.) = 440 (1.00), 535 (0.09), 583 (0.06), 624 (0.07), 688 (0.08) nm.

Pt(II)-tetra-(4-bromophenyl)-cyclohexenoporphyrin (PtTPCHPBr$_4$, A2). The crude product (700 mg crude, 100 mg pure product, calculated using Lambert Beer law, $\varepsilon = 250\,000\ M^{-1}\ cm^{-1}$ for the Soret band at 440 nm) was dissolved in TMB (60 ml) and heated to 150 °C. $Pt(C_6H_5CN)Cl_2$ (90 mg, 0.192 mmol) was pre-dissolved in a small volume of TMB and was added to the reaction mixture. The formed HCl was removed by bubbling N_2 through the reaction mixture. The reaction progress was monitored *via* UV-Vis spectra. After 1 h, the reaction was cooled and the insoluble products (metallic platinum) removed by filtration. The filtrate was refluxed with 45 mg $Pt(C_6H_5CN)Cl_2$. After the completion of the reaction, 50 ml hexane were added and the product was purified *via* chromatography on silica-gel (eluent: hexane/DCM, 2/1, v/v). Product fractions were determined *via* UV-Vis absorption spectra (see Fig. S1, ESI†). Yield: 52 mg, 51%. ^{1}H NMR (300 MHz, $CDCl_3$) δ 7.92 (d, J = 8.2 Hz, 8H), 7.81 (d, J = 8.1 Hz, 8H), 2.36–2.30 (m, 16H), 1.54–1.50 (m, 16H). MALDI: *m*/*z*: [M+] calc. for $C_{60}H_{48}Br_4N_4Pt$: 1340.0232; found, 1340.0132. UV-Vis (acetone): λ_{max} (rel. int.) = 410 (1.00), 523 (0.07), 558 (0.09) nm.

Pt(II) tetra-(4-bromophenyl)-tetrabenzoporphyrin (PtTPTBPBr$_4$, 3a). The platinated complex **A2** (194.5 mg, 0.169 mmol) was heated to reflux in 250 ml toluene. DDQ (385 mg, 1.696 mmol) was added. The red solution turned dark green after 5 minutes. Reaction progress was monitored using UV-Vis spectroscopy. After completion of the reaction, the green organic phase was washed three times with 10 wt% Na_2SO_3 solution. The solvent was removed under reduced pressure. Yield: 175 mg, 78%. ^{1}H NMR (300 MHz, benzene-d6) δ 7.79–7.70 (d, 8H), 7.68–7.61 (d, 8H), 7.34–7.26 (m, 8H), 7.08–7.00 (m, 8H). MALDI *m*/*z*: [M+] calc. for C60H32Br4N4Pt, 1323.898; found, 1323.903. UV-Vis (acetone): λ_{max} (rel. int.) = 428 (1.00), 566 (0.10), 615 (0.57) nm.

Zn-tetra-4-bromophenyl-tetrabenzoporhyrin (ZnTPTBPBr$_4$, B1a). Zn-4-bromophenylaetate (6.330 g, 13.60 mmol), 4-bromophenylacetic acid (11.699 g, 54.40 mmol) and 1,2-dicyanobenzene (6.971 g, 54.40 mmol) were mixed and homogenized using a mortar. The solid mixture was split into equal portions of roughly 700 mg, placed into 2.5 ml Supelco® vials and compressed. The vials were sealed with a metal screw cap, placed into a pre-heated metal block at 140 °C. The reagents were heated to a temperature of 280 °C and left to react for 40 minutes while stirring and subsequently left to cool. The melt in each vial was dissolved in acetone. The dye was precipitated by adding a three-fold volume of EtOH–water (1/1, v/v) mixture. This operation was repeated three times. The product was further purified on an Al_2O_3 column. Yield: 974 mg, 6%. UV-Vis (DCM): λ_{max} (rel. int.) = 464 (1.00), 607 (0.06), 656 (0.22) nm.

Tetra-4-bromophenyl-tetrabenzoporhyrin (H$_2$TPTBPBr$_4$, B2a). $ZnTPTBPBr_4$ (500 mg, 0.419 mmol) was dissolved in 1 ml of acetone and methanesulfonic acid (3.82 g, 39.80 mmol) was added. The solution was stirred for 15 minutes at room temperature resulting in a color change from green to brown-red. The product was precipitated with water, and re-dissolved in acetone. Precipitation was repeated three times until the protonated form of the free ligand was no longer detectable in the absorption spectra (characteristic band at 504 nm, see Fig. S2, ESI†). The metal-free porphyrin was dried at 65 °C. Yield: 463 mg, 98%. UV-Vis (DCM): λ_{max} (rel. int.) = 463 (1.00), 686 (0.06), 630 (0.13), 698 (0.04) nm.

Pt(II)-tetra-4-bromophenyl-tetrabenzoporhyrin (PtTPTBPBr$_4$, 3a). The ligand **B2a** (200 mg, 0.176 mmol) was dissolved in 200 ml TMB. The solution was heated to reflux at 170 °C. $Pt(C_6H_5CN)Cl_2$ (167 mg, 0.354 mmol) was added in small pre-dissolved portions (0.3 eq. in TMB) over 4 hours. After cooling, the product was purified on an Al_2O_3 column. Finally, the product was dissolved in a small volume of acetone and precipitated in a five-fold volume hexane and dried at 60 °C. Yield: 105 mg, 45%. ^{1}H NMR (300 MHz, benzene-d6) δ 7.78–7.70 (m, 8H), 7.69–7.60 (m, 8H), 7.36–7.26 (m, 8H), 7.07–6.99 (m, 8H). MALDI *m*/*z*: [M+] calc. for $C_{60}H_{32}Br_4N_4Pt$, 1323.898; found, 1323.892. UV-Vis (DCM): λ_{max} (rel. int.) = 431 (1.00), 569 (0.08), 619 (0.64) nm.

Pt(II)-5-(4-bromophenyl)-10,15,20-tri(phenyl)-tetrabenzoporhyrin (PtTPTBPBr, 3b). Compounds **B1b**, **B2b** and **3b** were synthesized in a similar way to the tetra-substituted benzoporphyrin. Their preparation is described in detail in the supplementary information.

Mono-styrene-substituted Pt(II)-tetraphenyl-tetrabenzoporhyrin (PtTPTBPStyr, 5). PtTPTBPBr (50 mg, 0.0460 mmol), 4-vinylphenylboronic acid (27.05 mg, 0.184 mmol) and K_2CO_3 (19.04 mg, 0.138 mmol) were added to 12.5 ml mixture of THF–toluene–H_2O (2/2/1 v/v/v) in a Schlenk flask. The reaction mixture was deoxygenated for 15 minutes by stirring it vigorously under argon. The catalyst $Pd(PPh_3)_4$ (1 mol%) was added and the reaction mixture was heated to 70 °C for 48 hours. After cooling down to room temperature, DCM was added and the mixture was washed with H_2O and sat. $NaHCO_3$ solution. The organic phase was dried over Na_2SO_4 and the solvent was removed under reduced pressure. The product was purified *via* column chromatography on silica gel (eluent: CH/DCM, 3/1, v/v). Yield: 27.7 mg, 53%. ^{1}H NMR (300 MHz, Chloroform-*d*) δ: 8.36–6.97 (m, 39H, benzoporphyrin + styrene (Ar)), 6.87 (dd, 0.8H styrene, CH_2–*CH*-Ar), 5.91 (d, 0.8H, styrene, *CH*$_2$–CH-Ar), 5.37 (d, 0.8H, styrene, *CH*$_2$–CH-Ar). MALDI: *m*/*z*: [M+] calc. for $C_{68}H_{42}N_4Pt$ (PtTPTBPStyr): 1108.308; found 1108.317. PtTPTBP (1006.257 calc.; 1006.256 found) and $PtTPTBPStyr_2$ (1210.351 calc.; 1210.371 found) are also detected.

Poly(styrene-*co*-4-vinylphenylboronic acid), 4. The synthetic concept is exemplified by the following synthesis. The exact composition for co-polymers with different monomer ratios is described in the supplementary information. Prior to the polymerisation styrene was filtered through Al_2O_3 to remove the stabilizer (4-*tert*-butylcatechol). Styrene (20 g, 22.002 ml, 0.192 mol, 0.999 eq.) and 4-vinylphenylboronic acid (28.4 mg,

0.192 mmol, 0.001 eq.) were placed in a dry Schlenk-flask under argon flow. The suspension was stirred for 20 minutes under argon flow before adding AIBN (315 mg, 1.92 mmol, 0.01 eq.). The reaction mixture was heated to 75 °C for 6 hours and a highly viscous mixture was formed. The polymer was dissolved in DCM (10 wt%) and purified by precipitating with methanol. Precipitation was repeated five times. The resulting white powder was dried in the oven at 75 °C. Yield: 7.409 g, 37%. Ph-$B(OH)_2$ content: 0.07 mol%. GPC data: Mn = 99 710 g mol^{-1}, Mw = 404 020 g mol^{-1}, Mz = 1 218 120 g mol^{-1}, PDI = 4.05.

Grafting of PtTPTBPBr (3b) to polymer 4. The synthetic concept is exemplified by the following synthesis. The used quantities for polymers with different amount of dye loading are described in the supplementary information. The co-polymer **4** (799 mg, 7.67 mmol), PtTPTBPBr (**3b**) (10 mg, 0.009 mmol) and K_2CO_3 (3 mg, 0.002 mmol) were dissolved in 20 ml toluene, 10 ml THF and 3 ml H_2O in a Schlenk-flask. The solution was deoxygenated by rapid stirring under strong argon flow for 10 min. The catalyst $Pd(PPh_3)_4$ (1 mol%) was added under argon. The Schlenk flask was closed, heated to 70 °C and left to react for 24 hours while stirring. To purify the product, the solution was added drop-wise to a five-fold volume of methanol, resulting in the formation of a green precipitate. The suspension was filtered through a paper filter and re-dissolved in dichloromethane to give a solution containing 10 wt% of polymer. This step of dissolving and precipitation was repeated three times, until no more dye could be observed in the washing solutions. The polymer (**6b**) was dried in the oven at 70 °C. Dye loading was calculated using Lambert Beers law, ε = 250 000 M^{-1} cm^{-1} at 430 nm in DCM = 0.41 wt%. Yield: 589 mg, 72%. GPC data: Mn = 118 950 g mol^{-1}, Mw = 457 810 g mol^{-1}, Mz = 1 320 760 g mol^{-1}, PDI = 3.85.

Co-polymerisation of PtTPTBPStyr (5) with styrene. Styrene was filtered through aluminum oxide to remove the stabilizer. 550 μl of styrene (500 mg, 4.481 mmol) and 5.5 mg of PtTPTBPStyr (1.01 wt%) were placed in a Schlenk tube and deoxygenated for 15 minutes. 7.9 mg AIBN (1 mol%) was added, the Schlenk was closed and heated to 70 °C for 2.5 hours. The polymer (**6b**) was dissolved in DCM and precipitated in a five-fold volume of methanol three times and dried in the vacuum oven at 60 °C. Dye loading was calculated using Lambert Beers law, ε = 250 000 M^{-1} cm^{-1} for the Soret band at 430 nm in DCM = 1.0 wt%. Yield: 340 mg, 60%. GPC data: Mn = 39 790 g mol^{-1}, Mw = 92 470 g mol^{-1}, Mz = 187 850 g mol^{-1}, PDI = 2.32.

Co-polymerisation of PtTPTBPStyr (5) with 1,1,1,3,3,3-hexafluoroisopropyl methacrylate. 760.3 μl 1,1,1,3,3,3-hexafluoroisopropyl methacrylate (990 mg, 4.19 mmol) were dissolved in 2 ml water-free THF in a Schlenk tube, 10 mg PtTPTBPStyr (1.0 wt%) were added and the solution was deoxygenated for 15 minutes. 0.68 mg AIBN (1 mol%) was added, the Schlenk was closed and heated to 70 °C for 22 hours. After completion of the reaction, 2 ml THF were added to the viscose polymer mixture and precipitated in 30 ml MeOH four times and the polymer (**7**) was dried in the drying cabinet at 60 °C. Dye loading was calculated using Lambert Beers law, ε = 250 000 M^{-1} cm^{-1} at 430 nm in THF = 0.64 wt%. Yield: 202 mg, 20%. GPC data: Mn = 57 000 g mol^{-1}, Mw = 68 500 g mol^{-1}, Mz = 83 220 g mol^{-1}, PDI = 1.20.

Co-polymerisation of PtTPTBPStyr (5) with styrene and maleic anhydride. Styrene was filtered through aluminum oxide to remove the stabilizer. 513 μl of styrene (466 mg, 4.481 mmol, 93 mol%), 33 mg of maleic anhydride (0.337 mol, 7 mol%) and 5.3 mg of PtTPTBPStyr (1.06 wt%) were placed in a Schlenk tube and deoxygenated for 15 minutes. 7.9 mg AIBN (1 mol%) was added, the Schlenk was closed and heated to 70 °C for 2.5 hours. The polymer (**8**) was dissolved in DCM and precipitated in a five-fold volume of methanol three times and dried in the vacuum oven at 60 °C. Dye loading was calculated using Lambert Beers law, ε = 250 000 M^{-1} cm^{-1} at 430 nm in DCM = 0.56 wt%. Yield: 340 mg, 60%. GPC data: Mn = 46 050 g mol^{-1}, Mw = 250 500 g mol^{-1}, Mz = 888 800 g mol^{-1}, PDI = 5.44.

Preparation of PSMA nanoparticles. The PSMA-copolymer **8** was dissolved in THF giving a 0.5 wt% solution. The cocktail was added controlled with a pipette to a two-fold volume of H_2O while stirring on a vortex with 1200 rpm. THF was allowed to evaporate for 2 hours under ambient air flow. Particle size: Z_{av} 85 nm, PDI 0.15. Zeta potential = −40.9 mV.

Preparation of sensor films. Sensor films of defined thickness were prepared by knife coating of "cocktails" onto PET foils using a Gardner 25 μm coating knife. The polystyrene-based "cocktails" typically contained 10 wt% of polymer dissolved in chloroform (HPLC-grade). The poly(1,1,1,3,3,3-hexafluoroisopropyl methacrylate)-based "cocktail" contained 30 wt% of the polymer in THF. After coating, the sensor films were dried for 24 hours at 70 °C to ensure complete removal of solvent before characterization.

Fiber-optic sensors. The cladding of the 1 mm PMMA fiber was removed with acetone. The core was coated by dipping the fiber in a "cocktail" containing 2 wt% of the polymer (1.0 wt% PtTPTBPStyr co-polymerised in polystyrene (**6b**)) in ethylacetate. The fiber was dried at 60 °C for 24 hours to remove the solvent. The tip of the fiber was cut off to ensure that the obtained signals resulted from side wall coating of the fiber. The sensor response was measured by dipping the fiber into a 2 wt% Na_2SO_3 solution.

Autoclavation experiments

100 mg of the sensor material PS co-polymerised with compound **5** or 1 mg $PtTPTBPBr_4$ (**3a**) and 100 mg PS were dissolved in 1.0 g HPLC grade chloroform. These sensor "cocktails" were coated onto PET and microscopy slides using a 25 μm coating knife. The sensors were dried at 60 °C for 12 h. The sensors were autoclaved (Sanoclav from Wolf, Germany) at 135 °C for 15 h and phosphorescence lifetimes were determined under air and nitrogen in regular intervals.

Photostability

Dye solutions in water-free DMF were illuminated with and LED array (617 nm) at the following settings: 7.0 W, 7.88 V, 882 mA (photon flux: 5500 μmol s^{-1} m^{-2}). After each measurement the cuvette was shortly unsealed and shaken to ensure oxygen saturation in the sample. The degradation was determined by calculating the average value of the three maximum absorption points in the Q-band.

Measurements

^{1}H NMR spectra were recorded on a 300 MHz instrument from Bruker. MALDI-TOF mass spectra were recorded on a Micromass TofSpec 2E in refectron mode at an accelerating voltage of +20 kV. Boronic acid content was determined using elemental analyses on a Spectro Ciros Vision ICP-OES after microwave assisted digestion on a Muliwave 3000 from Anton Paar (Austria). Absorption measurements were performed on a Cary 50 UV-Vis spectrophotometer from Varian. Luminescence spectra were acquired on a Fluorolog-3 luminescence spectrometer (Horiba). Relative luminescence quantum yields were determined according to Crosby and Demas[45] using platinum(II) tetraphenyltetrabenzoporphyrin ($\Phi = 0.51$)[34] as a reference. The samples were de-oxygenated in a screw-cap cuvette (Hellma) by bubbling argon through the solutions for 25 min. GPC measurements for determination of molecular weights and the PDI of the polymers were carried out in tetrahydrofuran (THF) using a Merck Hitachi L6000 pump, separation columns of Polymer Standards Service (5 μm grade size) and a refractive-index detector from Wyatt Technology. For calibration Polystyrene Standards purchased from Polymer Standard Service were used. Particle size and zeta potential were measured using a Zetasizer Nano-ZS from Malvern Instruments.

Calibration of the polystyrene-based sensors (3 sensors were measured to obtain average values) was performed in the frequency-domain using a SR830 DSP lock-in amplifier (Stanford Research Systems). Excitation light from a 435 nm LED obtained from Roithner, Austria was filtered through a BG12 filter obtained from Schott, Germany. The excitation light was sinusoidally modulated at a frequency of 5 kHz and guided to the sensor film using a bifurcated fiber bundle. The emitted light was guided back to a photomultiplier unit (H5701-02) obtained from Hamamatsu, Japan. The emission light was filtered through an RG 9 filter obtained from Schott. Calibration of all other sensors and the stability tests were performed using a Firesting oxygen meter from Pyroscience (Germany). The modulation frequency of 4 kHz was used. The gas mixtures were adjusted with a custom-built gas-mixing device based on mass-flow controllers from MKS (http://www.mksinst.com) and Voegtlin (Switzerland, http://www.red-y.com) by mixing nitrogen and compressed air. The temperature was kept constant at 25 °C with a HAAKE DC50 or ThermoHAAKE K10 thermostat.

Acknowledgements

The support from Josefine Hobisch and Robert Saf (Institute of Chemistry and Technology of Materials, TU Graz), Herbert Motter and Eveline Maier (Institute of Analytical Chemistry and Food Chemistry) is gratefully acknowledged. The work was financially supported by ERC Project "Oxygen" – grant number 267233.

References

1 R. I. Dmitriev and D. B. Papkovsky, *Cell. Mol. Life Sci.*, 2012, **69**, 2025–2039.
2 D. B. Papkovsky and R. I. Dmitriev, *Chem. Soc. Rev.*, 2013, **42**, 8700–8732.
3 S. Schreml, R. J. Meier, O. S. Wolfbeis, T. Maisch, R.-M. Szeimies, M. Landthaler, *et al.*, *Exp. Dermatol.*, 2011, **20**, 550–554.
4 J. Lecoq, A. Parpaleix, E. Roussakis, M. Ducros, Y. G. Houssen, S. A. Vinogradov, *et al.*, *Nat. Med.*, 2011, **17**, 893–898.
5 M. Staal, S. M. Borisov, L. F. Rickelt, I. Klimant and M. Kühl, *J. Microbiol. Methods*, 2011, **85**, 67–74.
6 A. Hempel, M. G. O'Sullivan, D. B. Papkovsky and J. P. Kerry, *LWT – Food Sci. Technol.*, 2013, **50**, 226–231.
7 A. Mills, *Chem. Soc. Rev.*, 2005, **34**, 1003–1011.
8 O. Kohls and T. Scheper, *Sens. Actuators, B*, 2000, **70**, 121–130.
9 O. S. Wolfbeis, *J. Mater. Chem.*, 2005, **15**, 2657–2669.
10 X. Wang and O. S. Wolfbeis, *Chem. Soc. Rev.*, 2014, **43**, 3666–3761.
11 B. D. MacCraith and C. McDonagh, *J. Fluoresc.*, 2002, **12**, 333–342.
12 B. Korzeniowska, R. Nooney, D. Wencel and C. McDonagh, *Nanotechnology*, 2013, **24**, 442002.
13 M. Quaranta, S. M. Borisov and I. Klimant, *Bioanal. Rev.*, 2012, **4**, 115–157.
14 H. Xiang, J. Cheng, X. Ma, X. Zhou and J. J. Chruma, *Chem. Soc. Rev.*, 2013, **42**, 6128.
15 D. B. Papkovsky, G. V. Ponomarev, W. Trettnak and P. O'Leary, *Anal. Chem.*, 1995, **67**, 4112–4117.
16 G. Khalil, M. Gouterman, S. Ching, C. Costin, L. Coyle, S. Gouin, *et al.*, *J. Porphyrins Phthalocyanines*, 2002, **6**, 135–145.
17 S. A. Vinogradov and D. F. Wilson, *J. Chem. Soc. Perkin Trans.*, 1995, 103–111.
18 M. A. Filatov, S. Baluschev, I. Z. Ilieva, V. Enkelmann, T. Miteva, K. Landfester, *et al.*, *J. Org. Chem.*, 2012, **77**, 11119–11131.
19 S. M. Borisov, G. Nuss and I. Klimant, *Anal. Chem.*, 2008, **80**, 9435–9442.
20 S. M. Borisov, G. Zenkl and I. Klimant, *ACS Appl. Mater. Interfaces.*, 2010, **2**, 366–374.
21 I. Dunphy, S. A. Vinogradov and D. F. Wilson, *Anal. Biochem.*, 2002, **310**, 191–198.
22 T. V. Esipova, A. Karagodov, J. Miller, D. F. Wilson, T. M. Busch and S. A. Vinogradov, *Anal. Chem.*, 2011, **83**, 8756–8765.
23 M. C. DeRosa, D. J. Hodgson, G. D. Enright, B. Dawson, C. E. B. Evans and R. J. Crutchley, *J. Am. Chem. Soc.*, 2004, **126**, 7619–7626.
24 M. C. DeRosa, P. J. Mosher, G. P. A. Yap, K.-S. Focsaneanu, R. J. Crutchley and C. E. B. Evans, *Inorg. Chem.*, 2003, **42**, 4864–4872.
25 B. Lei, B. Li, H. Zhang, L. Zhang and W. Li, *J. Phys. Chem. C*, 2007, **111**, 11291–11301.
26 Z. Wang, A. r. McWilliams, C. E. B. Evans, X. Lu, S. Chung, M. a. Winnik, *et al.*, *Adv. Funct. Mater.*, 2002, **12**, 415–419.
27 H. Zhang, B. Lei, W. Mai and Y. Liu, *Sens. Actuators, B*, 2011, **160**, 677–683.

28 H. Zhang, B. Li, B. Lei, W. Li and S. Lu, *Sens. Actuators, B*, 2007, **123**, 508–515.
29 Y. Tian, B. R. Shumway, W. Gao, C. Youngbull, M. R. Holl, R. H. Johnson, *et al.*, *Sens. Actuators, B*, 2010, **150**, 579–587.
30 Y. Tian, B. R. Shumway and D. R. Meldrum, *Chem. Mater.*, 2010, **22**, 2069–2078.
31 K. Koren, S. M. Borisov and I. Klimant, *Sens. Actuators, B*, 2012, **169**, 173–181.
32 M. Obata, N. Matsuura, K. Mitsuo, H. Nagai, K. Asai, M. Harada, *et al.*, *J. Polym. Sci., Part A: Polym. Chem.*, 2010, **48**, 663–670.
33 S. M. Borisov, P. Lehner and I. Klimant, *Anal. Chim. Acta*, 2011, **690**, 108–115.
34 S. M. Borisov, G. Nuss, W. Haas, R. Saf, M. Schmuck and I. Klimant, *J. Photochem. Photobiol., A*, 2009, **201**, 128–135.
35 O. S. Finikova, A. V. Cheprakov, I. P. Beletskaya, P. J. Carroll and S. A. Vinogradov, *J. Org. Chem.*, 2004, **69**, 522–535.
36 C. Borek, K. Hanson, P. I. Djurovich, M. E. Thompson, K. Aznavour, R. Bau, *et al.*, *Angew. Chem., Int. Ed.*, 2007, **46**, 1109–1112.
37 J. Lindsey, H. Hsu and I. Schreiman, *Tetrahedron Lett.*, 1986, **27**, 4969–4970.
38 S. M. Borisov and I. Klimant, *Dyes Pigm.*, 2009, **83**, 312–316.
39 K. Ichimura, M. Sakuragi, H. Morii, M. Yasuike, M. Fukui and O. Ohno, *Inorg. Chim. Acta*, 1991, **182**, 83–86.
40 X. Cui, J. Zhao, P. Yang and J. Sun, *Chem. Commun.*, 2013, **49**, 10221.
41 M. J. Currie, J. K. Mapel, T. D. Heidel, S. Goffri and M. A. Baldo, *Science*, 2008, **321**, 226–228.
42 J. Zhao, W. Wu, J. Sun and S. Guo, *Chem. Soc. Rev.*, 2013, **42**, 5323–5351.
43 S. M. Borisov, T. Mayr, G. Mistlberger, K. Waich, K. Koren, P. Chojnacki, *et al.*, *Talanta*, 2009, **79**, 1322–1330.
44 E. R. Carraway, J. N. Demas, B. A. DeGraff and J. R. Bacon, *Anal. Chem.*, 1991, **63**, 337–342.
45 G. A. Crosby and J. N. Demas, *J. Phys. Chem.*, 1971, **75**, 991–1024.